

## Identification of Ancient Burial Ceramics from Ban Muang Bua, Northeastern Thailand using SEM-EDS and SR XTM

Nontarat Nimsuwan<sup>1</sup>, Jirapan Dutchaneephet<sup>2</sup>, Phakkhananan Pakawanit<sup>3</sup>, Pisutti Dararutana<sup>4</sup> and Krit Won-in<sup>1\*</sup>

<sup>1</sup> Department of Earth Science, Faculty of Science, Kasetsart University, Bangkok 10900, Thailand

<sup>2</sup> Thailand National Sports University Phetchabun, Phetchabun 67000 Thailand

<sup>3</sup> Synchrotron Light Research Institute, Nakhon Ratchasima 30000 Thailand

<sup>4</sup> Retired Army Officer, Royal Thai Army, Bangkok 10900 Thailand

---

### Abstract

It is revealed that the ancient ceramics found at Ban Muang Bua located in northeastern Thailand, are one of the Thung Kula Ronghai ceramics. They are produced as burial goods for funeral offerings or used as the burial jars and daily-used ceramics. Shreds of these samples are analyzed of the elemental composition and structure using a scanning electron microscope coupling with energy dispersive X-ray fluorescent spectroscopy (SEM-EDS). X-ray tomographic microscopy (SR XTM) based on synchrotron radiation is performed to investigate the three-dimensional (3-D) structure. The elements present as major, minor and trace elements, such as carbon (C), silica (Si), aluminum (Al), phosphorus (P), calcium (Ca), potassium (K), titanium (Ti), iron (Fe), sodium (Na), magnesium (Mg), and Zinc (Zn), were identified to the origin of the samples as the fingerprint. The 3-D tomographic images revealed the internal configuration of these samples. It was shown that the combination of various analytical methods is a powerful tool with which to answer the questions posed by archaeology.

**Keywords:** ancient ceramics, Ban Muang Bua, SEM-EDS, SR XTM

---

### Article Info

Received 15<sup>th</sup> October 2019

Accepted 29<sup>th</sup> November 2019

Published 2<sup>nd</sup> December 2019

\*Corresponding author: Krit Won-in; e-mail: kritwonin@gmail.com

Copyright Malaysian Journal of Microscopy (2019). All rights reserved. ISSN: 1823-7010

eISSN: 2600-7444

## Introduction

The investigation of cultural heritage such as ceramics, mortars, glasses, etc., is a multidisciplinary work that incorporates researchers from various fields of study. Archaeological considerations are important to classify the aesthetic styles and to identify the historical and geographical context in which an artistic object was made. The identification of compositional characteristics specific to a certain set of ancient pottery has led to information about production techniques, production sites, and the dates of objects under investigation [1, 2]. Previous studies in Thailand have been carried out in order to analyze the archaeological ceramics using various techniques. The unearthed potsherds came from Au-Thong site, Suphan Buri (Central province of Thailand) were examined with a multi-analytical approach, including petrographic, mineralogical and chemical composition investigations was carried out by means of micro-beam X-ray fluorescence spectroscopy ( $\mu$ -XRF), optical microscope (OM), scanning electron microscope coupled with energy dispersive X-ray fluorescence spectroscopy (SEM-EDS) and particle induced X-ray emission spectroscopy (PIXE). X-ray diffractometer (XRD) was also performed to confirm the presence of clay minerals. The composition analysis showed the heterogeneous matrices which were commonly associated with a high concentration of elements such as Ca, Fe, Al or Ti that used to be the pottery characterization [3].  $\mu$ -XRF based on synchrotron radiation was applied to identify the elemental composition in the specific areas of the Wiangkalong underglaze painted black-on-white wares. The detected elements could be used as the fingerprint element [4].

Tomographic microscopy is a powerful non-destructive technique used to visualize and study the three dimensional internal structure and material properties of a variety of opaque samples [5-8]. It is an excellent tool for the investigation of a wider range of samples such as materials [9-12], earth sciences [13], fossils [14-19], archaeology [20-25], food [26], pharmaceutical [27] and environmental [28].

Ban Muang Bua is located in Roi Et province, northeastern Thailand. It is identified that the Ban Muang Bua prehistoric ceramics are the earthenware which originated from the Thung Kula Ronghai cultural group that dated around 1500 BC to 500 AD. These ceramics are categorized into 4 forms, such as the large burial jar used as the capsule jar burial, daily used slipped pot, daily used cord-marked pot, and low-fire earthenware, as shown in Figure I [29].

It is well known that clay is the raw material for pottery production. It mainly consists of fine particles and minerals that are primarily from resisting weathering igneous rocks.



Figure I Ban Muang Bua burial ceramic samples from Roi Et province, northeastern Thailand

## Materials and methods

Set of potsherd samples which collected from the ancient ceramic fragments excavated at Ban Muang Bua archaeological site in Roi Et province (northeastern Thailand), were characterized with the aim of obtaining information that would lead to identifying the microstructure and elemental composition, and the matrices of the samples by the means of SEM-EDS and SR XTM. Eight samples are labelled as MB001, MB002, MB003, MB005, MB007, MB008, MB009 and MB010.

Microstructure and elemental composition were characterized using a scanning electron microscope (SEM) QUANTA 450 (FEI Company, USA) coupled with energy dispersive X-ray spectrometer (EDS) X-Max (Oxford Instruments, UK) at the Science Equipment Center of Faculty of Science (Kasetsart University, Thailand). The SEM system was operated at 15 kV, and magnification of 25X to 500X. Semi-quantitative analysis of XRF spectra was performed using the INCA program (Oxford Instruments, UK). In each sample, three X-ray spectra were corrected at different positions, as shown in figure 2.

Synchrotron radiation X-ray tomographic microscopy (SR XTM) was carried out at the XTM beamline (BL1.2W), SLRI Thailand. For a complete dataset, X-ray projectors of each specimen were collected for 180° with 0.1° angular increment. In order to minimize the scattering and beam hardening artifacts, polychromatic X-rays were attenuated with 400 µm-thick aluminum foil to allow X-ray energy higher than 7 keV for X-ray imaging. The X-ray images were collected

on a CMOS camera with a pixel size of 0.7 microns. The data were then pre-processed and reconstructed in three dimensions based on a filtered-back projection algorithm using Octopus Reconstruction software. The 3-D segmentation and analysis of pores and grains along the volume were determined using Octopus Analysis software.

## Results and discussion

The chemical composition data obtained by EDS were given in Table I. It was found that all samples showed the detected elements, such as Si, Al, P, K, Ca, Ti, and Fe, while Na, Mg, Cl, and Zn were presented in some sample. The variation in the percentage of the elemental composition indicated that the raw materials were characteristically different in nature.

Table I The elemental composition of samples using EDS

Sample		Elemental composition using EDS (wt%)												
		C	O	Na	Mg	Al	Si	P	Cl	K	Ca	Ti	Fe	Zn
MB001	#1	5.61	51.41	N/D	N/D	4.26	34.98	1.82	N/D	0.24	0.50	0.28	0.85	0.04
	#2	7.57	49.27	0.21	N/D	3.77	35.44	1.78	0.10	0.31	0.49	0.31	0.77	N/D
	#3	9.88	49.82	N/D	0.10	4.76	31.28	2.03	N/D	0.26	0.58	0.38	0.75	0.16
MB002	#1	2.13	48.17	N/D	0.19	8.73	37.18	0.39	N/D	0.33	0.25	0.58	2.07	N/D
	#2	4.27	52.24	N/D	N/D	6.91	33.49	1.11	N/D	0.30	0.27	0.33	1.08	N/D
	#3	1.47	53.64	N/D	0.07	7.57	33.97	1.14	N/D	0.29	0.23	0.40	1.22	N/D
MB003	#1	3.28	50.19	N/D	N/D	4.11	39.79	1.05	N/D	0.10	0.26	0.34	0.89	N/D
	#2	3.88	50.92	N/D	N/D	4.78	37.18	1.71	N/D	0.16	0.29	0.29	0.78	N/D
	#3	4.04	54.47	N/D	0.09	5.00	33.37	1.25	N/D	0.21	0.28	0.34	0.96	N/D
MB005	#1	4.70	48.63	N/D	N/D	0.99	45.19	N/D	N/D	0.29	N/D	N/D	0.20	N/D
	#2	3.02	54.55	0.12	N/D	7.85	30.91	1.27	N/D	0.30	0.37	0.53	1.08	N/D
	#3	4.62	53.28	N/D	N/D	7.88	29.60	1.55	N/D	0.27	0.47	0.34	1.98	N/D
MB007	#1	3.73	58.49	N/D	N/D	5.62	28.60	0.65	N/D	0.27	1.00	0.22	1.41	N/D
	#2	3.65	52.69	N/D	0.10	4.75	35.92	0.38	N/D	0.26	0.83	0.22	1.20	N/D
	#3	5.72	46.62	N/D	0.15	6.66	36.39	0.26	N/D	0.47	1.49	0.46	1.78	N/D
MB008	#1	7.57	52.29	N/D	N/D	6.19	30.97	1.25	N/D	0.18	0.24	0.38	0.92	N/D
	#2	3.86	53.11	N/D	N/D	7.09	33.40	0.72	N/D	0.19	0.20	0.46	0.97	N/D
	#3	1.84	53.32	N/D	N/D	7.65	33.39	1.12	N/D	0.26	0.34	0.88	1.69	N/D
MB009	#1	7.68	53.50	0.18	0.26	5.02	30.58	0.79	N/D	0.47	0.49	0.31	0.72	N/D
	#2	1.91	51.45	N/D	N/D	4.73	39.37	0.57	N/D	0.37	0.53	0.22	0.85	N/D
	#3	12.48	48.99	0.34	0.14	5.32	29.47	0.47	0.20	0.51	0.59	0.41	1.09	N/D
MB010	#1	2.53	54.41	0.15	N/D	5.07	34.18	1.27	0.09	0.40	0.65	0.26	0.99	N/D
	#2	3.71	53.26	0.15	N/D	5.54	34.63	0.75	N/D	0.47	0.49	0.28	0.72	N/D
	#3	5.36	49.44	0.21	0.13	5.28	34.38	1.83	0.20	0.57	0.81	0.47	1.33	N/D

N/D denotes that it is no element detected; no element and/or below the lowest level limit detection of EDS.

Si and Al were found as the major element, but variation in the percentage of the composition. Their percentage were ranged from 28.60 to 45.19 % and 0.99 to 8.70, respectively. Ca content detected the <0.10 – 1.49 % range, while K ranged from approximately 0.18 – 0.57%. Because of other elements found in all samples suggested that the clays might be procured from the same area for making pottery products. The low percentage of Ca and K indicated that these samples were fired at low temperatures [30-31].

The presence of Fe in the original earthen clays which used as the raw materials affected the red color of pottery.

It is revealed the source of P contamination in the ancient potteries can be different, such as minerals, bone ashes that added into the clay paste, foods contained in the potteries during their use and burial environment [32-34]. P which was presented in all samples assumed by the burial contamination.

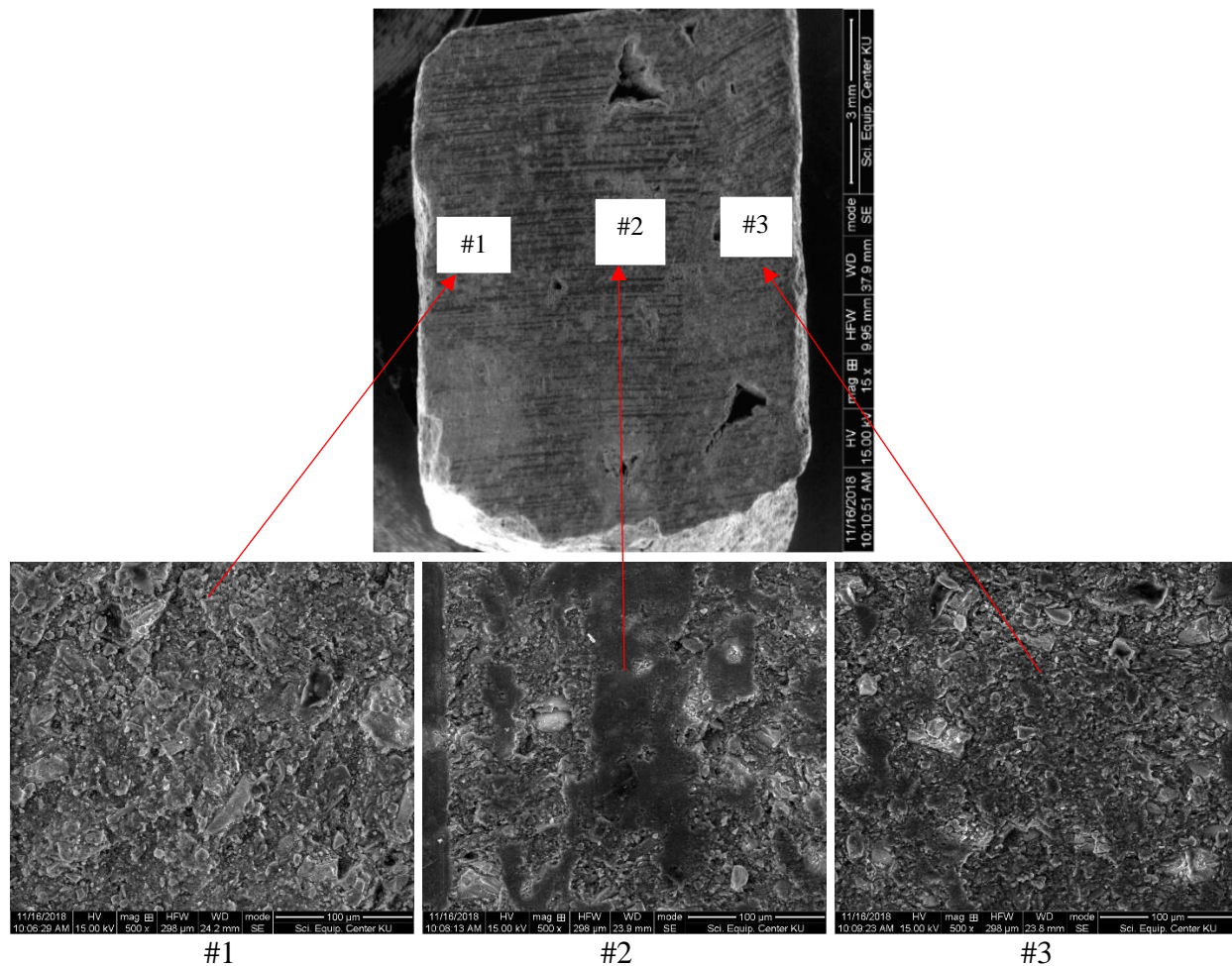


Figure II SEM micrographs of a sample from MB001, outer layer (#1), body (#2) and inner layer (#3)

It is well known that ceramics are an inorganic and non-metallic solid produced by the action of firing and cooling processes. The SEM was employed to investigate the specific surface morphological features of the samples. The micrographs gave a direct view of the densification which was a very informative feature of the technology used for the ancient pottery fabrication. The surface of the samples contained irregularly plate-like granules with a variety in size, as shown in Figure II. They showed three layers, such as outer layer (#1), body (#2), and inner layer (#3) which covered with a composite material composing of crystalline and non-crystalline phases. The different layers both outer and inner were used for sealing and wear resistance.

SR XTM represented a powerful non-destructive investigation technique and capable of displaying in a 3-D view of the volume and internal structure of the investigated samples. The 3-

D reconstructed results revealed not only the surface information but also the core structure of the samples [23-24, 35]. Figure III showed one slice that was extracted from the imagery of the sample, which contained isolated large-sized pores and cracks traces.

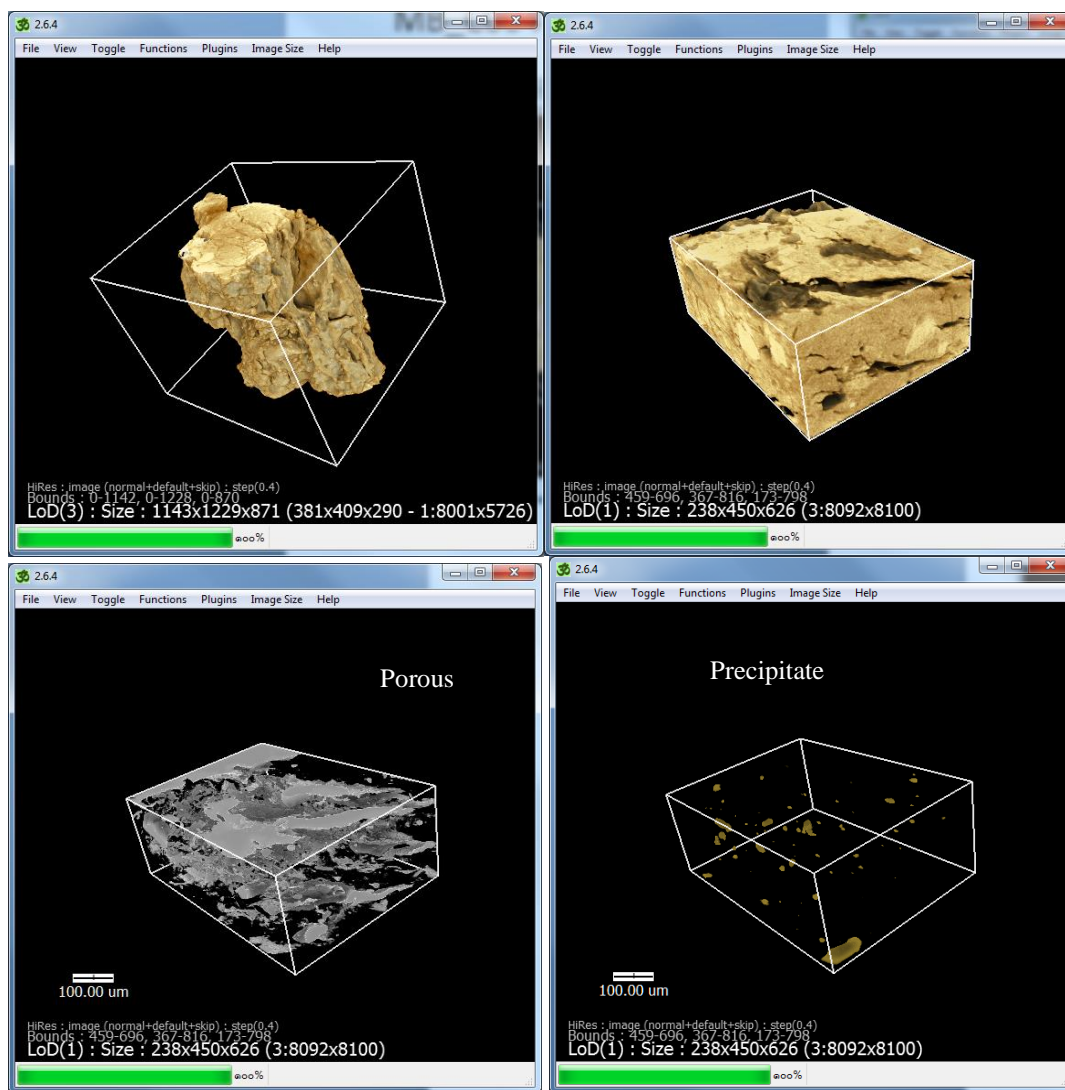


Figure III Tomographic images of sample MB004

The advanced works were carried out by using more synchrotron radiation facilities, such as micro-beam X-ray fluorescence spectroscopy ( $\mu$ -XRF), X-ray absorption spectroscopy (XAS), and X-ray photoemission spectroscopy (XPS). It was found that iron (Fe) was distributed in different regions both body and coating. Figure III, it was also shown that the dense region contained  $\text{Fe}^{2+}$ , while more oxygen permeable ones contained  $\text{Fe}^{3+}$  in the form of maghemite ( $\alpha\text{-Fe}_2\text{O}_3$ ). It is revealed that the  $\text{Fe}^{3+}$  presentation and distribution are formed during the re-oxidation of  $\text{Fe}^{2+}$ , which is significant to some of the firing process. Moreover, the presence of  $\text{Fe}^{3+}$  on the coating surfaces and interface between the body and the coating layers, the tendrils like precipitates from oxidized to reduced areas were delicious and very slightly basis that these samples were once reduced and then partially re-oxidized.

It was found that the micrographs of these samples using both SEM and SRXTM revealed a broad distribution of agglomerates of fine particles with porous structures

## Conclusion

In this study, the goal is to first ever to attempt the spectroscopic characterization of the ancient burial ceramics produced in the kiln of Ban Muang Bua, Roi Et Province (northeastern Thailand).

The SEM-EDS is an essential technique for the characterization of the ancient pottery in the forms of the elemental composition and microstructure. The SR XTM studied reported in this paper revealed the internal structure of the ancient ceramic artifacts under archaeological consideration. The imaging technique using X-ray tomography has yielded interesting details about the structure of the archaeological objects.

The information provided by these techniques consisted of the elemental composition and the distribution, shape, and dimensions of the samples.

## Acknowledgment

Department of Earth Sciences, Faculty of Sciences at Kasetsart University (Bangkok, Thailand) kindly thanks for providing the samples and partly funding. The BL1.2W at SLRI (Nakhon Ratchasima, Thailand) and the Science Equipment Center of Faculty of Science (Kasetsart University, Bangkok, Thailand) also thank for supporting the SR XTM and SEM-EDS facilities, respectively.

## Author Contributions

All authors contributed toward data analysis, drafting and critically revising the paper and agree to be accountable for all aspects of the work.

## Disclosure of Conflict of Interest

The authors have no disclosures to declare.

## Compliance with Ethical Standards

The work is compliant with ethical standards.

## References

- [1] Chaivari, C, Martini, S.E., Vandini, M. (2001) Thermoluminescence characterization and dating feasibility of ancient glass mosaic. *Quaternary Sci. Reviews.* 20 967.
- [2] Barilaro, D., et.al. (2006) Characterization of ancient amphorae by spectroscopic techniques. *Vibrational Spectroscopy.* 42 381.
- [3] Dararutana, P., et.al. (2011)  $\mu$ -XRF study on unearthed ancient pottery at Au-Thong. Thailand. *Acta Crystallographica Sections A.* 67 C763.
- [4] Won-in, K., Tancharokorn, S., Dararutana, P. (2017) Microanalysis study on Wiangkalong ancient pottery. *Journal of Physics Conference Series.* 901 012024.

- [5] Stampanoni, M., et.al. (2002) An X-ray tomographic microscope with submicron resolution. *Acta Physica B*. 33 463.
- [6] Marone, F., et.al. (2009) X-ray tomographic microscopy at TOMCAT. *Journal of Physics: Conference Series*. 189 012042.
- [7] Marone, F., et.al. (2011) Synchrotron-based X-ray tomographic microscopy at the Swiss Light Source for industrial applications. *Synchrotron Radiation News*. 24 24.
- [8] Pavel, C., et.al. (2014) X-ray tomography studies of prehistoric ceramic artifacts. *International Journal of Modern Physics: Conference Series*. 27 1460135.
- [9] Eller, J., et.al. (2011) Progress in in-situ X-ray tomographic microscopy of liquid water in gas diffusion layers of PEFC. *Journal of the Electrochemical Society*. 158 B963.
- [10] Puncrebutr, C., et.al. (2014) Coupling in site synchrotron X-ray tomographic microscopy and numerical simulation to quantify the influence of intermetallic formation on permeability in aluminium-silica-copper alloys. *Acta Materialia*. 64 316.
- [11] Cordes, N.L., et.al. (2015) Synchrotron-based X-ray computed tomography during compression loading of cellular materials. *Microscopy Today*. 12.
- [12] Sloof, W.G., et.al. (2016) Repeated crack healing in MAX-phase ceramics revealed by 4D in situ synchrotron X-ray tomographic microscopy. *Scientific Reports*. 6 23040.
- [13] Madonma, C., et.al. (2013) Synchrotron-based X-ray tomographic microscopy for rock physics investigations. *Geophysics*. 78 D53.
- [14] Schmidt, D.N., et.al. (2013) Linking evolution and development: Synchrotron radiation X-ray tomographic microscopy of planktic foraminifers. *Palaeontology*. 56 741.
- [15] Scott, A.C., et.al. (2009) Scanning electron microscopy and synchrotron radiation X-ray tomographic microscopy of 330 million year old charcolified seed fern fertile organs. *Microsc.Microanal.* 15 166.
- [16] Motchurova-Dekova, N., Harper, D.A.T. Synchrotron radiation X-ray tomographic microscopy (SRXTM) of brachiopod shell interiors for taxonomy: Preliminary report. *Annales Geologiques de la Peninsule Balkanique*. 71 109.
- [17] Kanitpanyacharoen, W., et.al. (2013) A comparative study of X-ray tomographic microscopy on shades at different synchrotron facilities: ALS, APS and SLS. *Journal of Synchrotron Radiation*. 20 1.
- [18] Kouchinsky, A., S Bengtoon, S. (2017) X-ray tomographic microscopy tighten affinity of the Early Cambrian Oymurania to the brachiopod stem group. *Acta Palaeontologica Polonica*. 62 39.
- [19] Kun, G.Z. Synchrotron X-ray tomographic microscopy reveals histology and internal structure of Galeaspida (Agnatha). *Vertebrata Palasiatica*. 56 93.
- [20] Roemich, H., et.al. Degradation phenomena on historic glass: Non-destructive characterization by synchrotron radiation. The 9<sup>th</sup> International Conference on NDT of Art, Jerusalem (Israel), 25-30 May 2008.
- [21] Sakdanawat, A., Attwood, D. (2010) Nanoscale X-ray imaging. *Nature Photonics*. 4 840.
- [22] Mizuno, S.T., Sugiyanna, J. (2011) Identification of wood of archaeological heritage by X-ray micro-CT imaging. *Spring 8 Research Fractions, Environmental Science*. 120.
- [23] Re, A., et.al. (2015) X-ray tomography of a soil block: A useful tool for the restoration of archaeological finds. *Heritage Science*. 3 1.
- [24] Zong, Y., et.al. (2017) Structural and compositional analysis of a casting mold sherd from ancient China. *Plos ONE*. 12(3) 1.

- [25] Cotte, M., et.al. (In press) Applications of synchrotron X-ray nano-probes in the field of cultural heritage. *Comptes Rendus Physique*.
- [26] Meirer, F., et.al. (2011) Three-dimensional imaging of chemical phase transformations at the nanoscale with full-field transmission X-ray microscopy. *J Synchrotron Radiat*. 18 773.
- [27] Agatston, A.S., et.al. (1990) Quantification of coronary artery calcium using ultrafast computed tomography. *J Am Coll Cardiol*. 15(4) 827.
- [28] Obst, M., Schmid, G. (2014) 3D Chemical Mapping: Application of Scanning Transmission (Soft) X-ray Microscopy (STXM) in Combination with Angle-Scan Tomography in Bio-, Geo-, and Environmental Sciences. *Electron Microscopy. Methods in Molecular Biology (Methods and Protocols)*, Vol 1117. Ed. By Kuo J. (Humana Press, NJ).
- [29] Sukkham, A. (2016) Re-cataloging SEACM Prehistoric Ceramic Collection. *Southeast Asian Ceramics Museum Newsletter*, IX(3) 1.
- [30] Krapukaityte, J., et.al. (2006) SEM and EDX characterization of ancient pottery. *Lithuanian Journal of Physics*. 46(3) 383.
- [31] Paranel, R., Meyvel, S. (2010) Microstructural and microanalytical study-(SEM) of archaeological pottery artefacts. *Rom.Journ.Phys*. 55(3-4) 333.
- [32] Pillay, A.E., et.al. (2000) Analysis of ancient pottery and ceramic objects using X-ray fluorescence spectrometry. *X-ray Spectrometry*. 29 53.
- [33] Maggetti, M. (2001) Chemical analyses of ancient ceramics: What for? *Chimia*. 55(11) 923.
- [34] Zlateva, B., Dumanov, B., Rangelov, M. (2018) Applications of soil phosphate analysis of activity areas at Doschkere, SE Bulgaria. *Journal of Historical Archaeology & Anthropological Sciences*. 3(1) 57.
- [35] Marie, E., Withers, P. (2014) Quantitative X-ray tomography. *Int.Mater.Rev*. 59 1.